Experimental Study of Ship Response due to Internal Viscous Cargo Motions

Virginie Baudry, Jean-Marc Rousset

Proceedings of the ASME 2018 37th International Conference on Ocean, Offshore & Arctic Engineering
OMAE2018
June 17-22, 2018, Madrid, Spain

OMAE2018-77502

EXPERIMENTAL STUDY OF SHIP RESPONSE DUE TO INTERNAL VISCOUS CARGO MOTIONS

Virginie Baudry
Ecole Centrale Nantes
LHEEA, CNRS 6598
Nantes, France

Jean-Marc Rousset
Ecole Centrale Nantes
LHEEA, CNRS 6598
Nantes, France

ABSTRACT

Potential liquefaction of some cargoes (Nickel ore, iron ore, …) is a major risk for the industry. The difficulties to simulate accurately the behaviour of these materials as well their interaction with a bulk carrier model lead to use highly viscous fluid. Such an experimental approach is presented in the paper. Roll responses of the ship model as well as details about the internal free surface behaviours are investigated for different loading conditions: solid cargo, fresh water and viscous fluids.

INTRODUCTION

The liquefaction is a phenomenon in which an apparent dry cargo material is abruptly transformed from a solid dry state to a fluid state. Some common materials currently transported on board bulk carriers, such as iron ore fines or Nickel ore are examples of materials that may liquefy.

On board bulk carriers, two major kinds of liquefaction may cause the vessel to list : (1) a global liquefaction phenomenon where the whole cargo suddenly begins to behave as a liquid cargo, with associated free surface consequences (metacentric height reduction), (2) a partial liquefaction phenomenon resulting in the shifting of the cargo. Both phenomena may generate a permanent list of the vessel and possible capsize.

Between 1988 and 2016, 23 bulk carrier incidents – among which 17 vessel losses - were assigned to liquefaction problems [1].

The limitation of liquefaction risk being a topic of major concern for the security of bulk carriers, the International Maritime Organization (IMO) improved the test methods commonly used to measure the Transportation Moisture Level. The International Maritime Solid Bulk Cargo Code (IMSBC) [2] provides mandatory rules to limit the risk of liquefaction inception. Especially, it specifies safe practices to ensure the safe transportation of liquefiable cargoes, and also includes since 2016 the modified Proctor Fagerberg tests designed to determine the Transportable Moisture Limit of Iron Ore Fines. Some other reports are however stating that the current regulations are not always cautiously followed [3].

Mandatory rules are therefore frequently being amended to reduce the risk of liquefaction, however, the lack of comprehension of liquefaction inception onboard still limits the impact of the current regulation. Many research topics are therefore currently developed to better understand both the liquefaction inception phenomenon and the impact of ore liquefaction on ship stability [4]. Zou et al [5] presented a numerical model to study the sloshing motion of a highly viscous fluid submitted to roll motion in a rectangular tank. In this 2D model, a finite volume method is used to solve the Navier-Stokes equations, and the level set method is implemented to describe the behaviour of the free surface. The external moment exerted on the ship due to liquid sloshing is investigated both numerically and experimentally, and an increase of the moment generated by the viscous fluid with time is reported. The authors therefore mentioned a phase lag affecting the ship roll angle due to the motions of the viscous fluid.

More recently, Zhang et al [6] investigated numerically the behaviour of Nickel Ore Slurries in a cargo hold, and also investigated on the phase lag between the liquefied cargo and the ship's motion for different cargo moisture contents. Baudry et al [8] studied experimentally the behaviour of highly viscous materials in cargo holds and also studied that phase lag depending on excitation frequency and amplitude through forced motion experiments.

Recent researches have therefore been focused on the behaviour of highly viscous non-Newtonian fluids in cargo holds with characteristics close to nickel ore slurries. The next step is to investigate on the ship response submitted to internal fluid motion. In the present paper, the coupled motion of highly viscous fluid with ship is studied, the internal fluid having rheological characteristics similar to the slurries modelled by Zhang et al.

EXPERIMENTAL INVESTIGATIONS

The main objective of the present experimental campaign is to analyse the response in waves of a ship submitted to internal non-Newtonian viscous cargo motions. The analysis of internal cargo motions would also bring elements for the comprehension of the global response and would therefore give tracks to understand the loss of stability experienced by some bulk carriers.

Ship model characteristics

The ship model is chosen according the following objectives:

- a global experimental set-up ensuring different noticeable ship responses with respect to the nature of the cargo, such as a solid cargo or liquid cargos of different viscosities;
- a ship roll period, inner tank dimensions and geometric arrangement similar to those described in [8];
- a loading configuration (displacement, KG) as constant as possible whatever the nature of the cargo.

The first objective can be reached by a set-up as simple as possible involving a reduced list of key parameters and reducing physical variabilities. The experiments are performed with a ship model having a unique cargo hold, without forward speed and subject to side waves. The mooring set-up is designed to restrain the drift and the yaw of the model without perturbation of the other degrees of freedom.

The second objective is leading to keep the 1:50 geometric scale and a simplified ship hold identical to the tank previously tested on the hexapod, with inner dimensions L_T 0.645 m x l_T 0.640m. The actual results would then enable a direct comparison with those presented in 2017.

The last objective is reached designing a box-like barge with symmetrical cylindrical bow and stern, hosting a typical prismatic bulk carrier hold in its middle. The main dimensions of the model and the corresponding ship are listed in Table 1.

The hull, without bilge keel, is made of rigid foam (density 0.65) and an internal aluminium structure supports the equipment and the ballast. The bottom and longitudinal walls of the tank are provided directly by the inner sides of the hull and the transverse walls are made of Perspex. The middle of the tank is also corresponding to the midship (FIGURE 1).

The ballast is made of lead weights. Their arrangement is adjusted with respect to the different loading configurations in order to keep the same global centre of gravity. The changes in roll periods are then only related to the nature of the cargo (liquid or solid).

Table 1. Ship model main characteristics

Scale	***1:50***	***1:1***
Length (m)	3.65	182.5
Breadth (m)	0.73	36.5
Depth (m)	0.40	20.0
Draught (m)	0.189	9.45
Δ (10^3 kg)	0.465	58 125
Including cargo mass (10^3 kg)	54.5	6 812

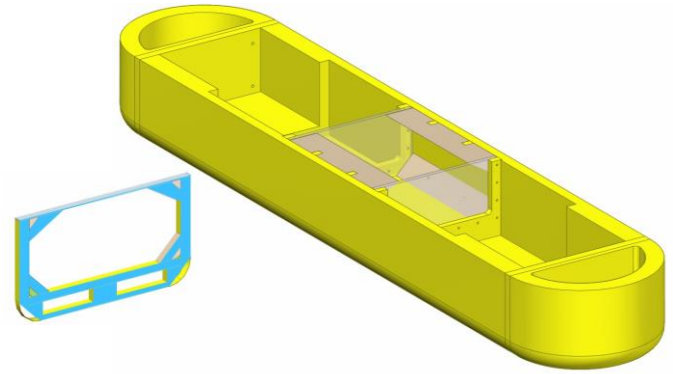

FIGURE 1. CAD VIEWS OF THE MODEL WITH THE TANK AT MIDSHIP AND THE TANK CROSS-SECTION (LEFT)

Experimental set-up and instrumentation

The model was positioned transversally in the middle of the ocean engineering tank, 18m away from the wave maker. The model is restraint by four soft mooring lines (FIGURE 2).

The soft mooring lines are composed of a thin dyneema rope and a steel linear spring (k=10 N/m). The barge mooring points are located at the bow and the stern on a longitudinal axis passing through the ship centre of gravity.

Reports on liquefaction incidents have shown that such kind of phenomenon mainly occur in transverse sea states. The experiments are then performed in transverse sea states (90° heading). The mooring lines are then 45° oriented from the longitudinal axis of the ship and attached on the wave tank walls.

Each fairlead is equipped with a lightweight uniaxial force transducer to measure the line tension. A similar pretension (around 6 N) is adjusted in each line through preliminary tests.

The model attitude is measured by a Qualisys optical motion tracking system which is calibrated in the measurement volume with a position uncertainty better than 1mm.

Two resistive wave probes measure the wave elevation respectively 1m upstream and downstream the model. A third one is located in the resting longitudinal axis of the model, far enough from it to be considered as a reference.

Eight capacitive wave probes are located inside the cargo hold to measure the internal free surface evolution. However the wave run-up on the inner lateral walls of the tank is not measured because of its prismatic shape. The probes 1, 4, 3 and 6 are located at 0.15m from the walls (FIGURE 3).

Both tank and internal wave probes are calibrated before the tests with the associated fluid (fresh water and/or viscous fluid). The model motions are measured simultaneously with the wave gauges, the line tensions and the wavemaker motions.

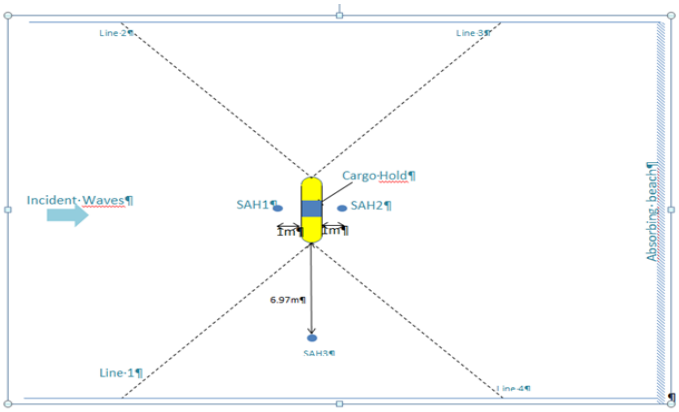

FIGURE 2. EXPERIMENTAL SET-UP IN THE WAVE TANK

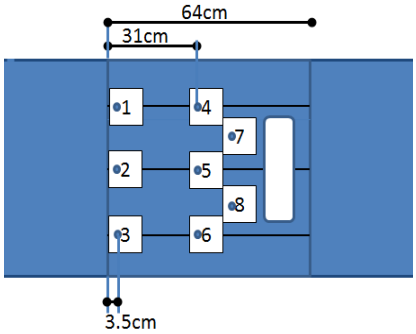

FIGURE 3. CAPACITIVE WAVE PROBES LOCATIONS IN THE TANK

Preparation and experimental program

The test program involves different steps to prepare the ship model for each cargo configuration (solid, water and viscous cargo).

The preparation consists in the ballasting of the model to reach the design water line and distributing the weights onboard to obtain the required centre of gravity through inclining tests on calm water.

For both water and viscous fluid configuration, the filling ratio of the internal tank is 46%, which corresponds to a standard filling ratio of bulk carrier cargo hold. The fluid depth in the tank is 0.135 m.

Experiments are performed in regular sea states, with wave periods from 6s to 18s at prototype scale (0.8 to 2.5 s at model scale), and wave heights of 1m, 2m and 4m at real scale (0.02, 0.04 and 0.08m at model scale). The regular waves are calibrated prior to the test campaign, without the ship model in the tank.

The evolution of the fluid viscosity during the experiments is taken into account and the test matrix is pragmatically adapted to identify the resonance period in roll for each configuration.

Viscous fluid properties

In the continuity of the hexapod measurement campaign performed in 2016 at Ecole Centrale de Nantes [8], the viscous fluid tested inside the ship tank is a cellulose-based drilling mud. This material has a high viscosity range with respect to its concentration, with an almost constant density close to fresh water. From a rheological point of view, the liquid is a non-Newtonian fluid with a pseudo-plastic behaviour.

For the present experiments, a concentration of 20g/l in fresh water is considered to comply with the forced motion tests performed with the hexapod.

Unlike the previous experiments, the mixture used in this campaign is unfortunately unstable and its viscosity is changing slowly with the time. The rheometer measurements are then performed twice during the campaign, on day 1 and on day 4. Results of these measurements are provided on FIGURE 4. Baudry et al. (2017) [8] are giving details on the characterization methods and the authors note that the fluid motions in the tank are inducing low shear rate: the left part of the curves is the region of interest, as indicated on FIGURE 4.

The main characteristics of the fluid are listed in Table 2. Its rheological analysis shows an effective reduction of viscosity at low shear rate by a factor of 3 at $\dot{\gamma} = 0.05$.

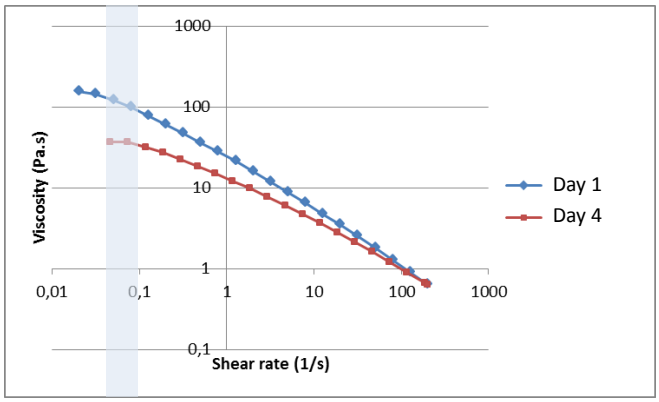

FIGURE 4. RHEOLOGICAL ANALYSIS OF THE VISCOUS MATERIAL

Table 2. Non-Newtonian viscous fluid main characteristics

Item	Unit	Viscous fluid-Day 1	Viscous fluid-Day 4
Type /Name		pseudo-plastic material	
Dilution with respect to water	g/l	20	20
Density	kg/m^3	1000	1000
Tank filling ratio		13.5cm (46%)	13.5cm (46%)
Herschel-Bulkley model coefficients - Extrapolated from experiments			
τ_{HB}	Pa	0	0
k_{HB}	kg/ms	9.63	21.69
n_{HB}	-	0.571	0.415
Apparent viscosity at $\dot{\gamma} = 0.05$	Pa.s	34.82	125.13
Experimental data			
Measured Viscosity at $\dot{\gamma} = 0.05$	Pa.s	37	120

Zhang et al [6] present a numerical model based on CFD solver to study the sloshing of Nickel ore slurries with three different moisture contents. In the case of low shear rates, the Herschel-Bulkley model is recommended: $\tau = \tau_{HB} + k_{HB}\dot{\gamma}^n$ with τ_{HB} : yield stress, k_{HB} : consistency index, $\dot{\gamma}$: the shear rate, n is the power law index. The authors assume the viscosity of the slurry can be defined by its apparent viscosity $\mu_a = \tau/\dot{\gamma}$

From our experimental data, τ_{HB} , k_{HB}, n as well as the apparent viscosity are evaluated (Table 2) and compared to the values of Zhang et al. reported in the flowing table.

The apparent viscosities of our liquid are coherent with the Nickel ore slurry 3 for the high value and Nickel ore slurry 2 for the lowest value.

Table 3. Low shear rate rheology parameters of nickel ore slurries studied by Zhang et al

Item	Density (kg/m^3)	τ_{HB} (Pa)	k_{HB} (kg/ms)	n_{HB}	Apparent Viscosity μ_{slurry} (Pa.s)
Nickel Ore Slurry 1, 60%water	1364	0.456	0.439	0.353	12.17
Nickel Ore Slurry 2, 50%water	1500	1.742	1.02	0.427	40.52
Nickel Ore Slurry3, 40%water	1667	4.741	3.774	0.565	108.71

RESULTS AND ANALYSIS

The results presented in this paper are given at model scale.

Free decay tests

Free decay tests on calm water are performed for each loading configuration (solid, water and viscous fluid cargo) in order to evaluate both roll natural frequency and damping.

The typical roll motion equation of a ship, without coupling with other degrees of freedom, can be written as follows [9]:

$$(I_x + A_r)\ddot{\varphi} + B_L\dot{\varphi} + B_{NL}\dot{\varphi}|\dot{\varphi}| + K\varphi = M_x(t)$$

$M_x(t)$ is the exciting moment, equals to zero in a calm water free decay test, I_x is the inertia in roll, A_r the added mass in roll, K the restoring coefficient, and B_L and B_{NL} respectively linear and quadratic damping coefficients.

Only linear damping is evaluated in this campaign, through decay tests with small angle of excitation. The non-dimensional roll motion equation becomes:

$$\ddot{\varphi} + 2\xi\omega_R\dot{\varphi} + \omega_R^2\varphi = 0$$

where $\xi = \frac{B_L}{B_c}$, and B_c is the critical damping defined as:

$B_c = 2\sqrt{(I_x + A_r)K}$.

Parameters ξ and T_R are experimentally evaluated from the roll measurements.

The results of roll periods evaluated for the different cargo configurations are given in the Table 4 and the main observations are given below:

- The highest value of the natural roll period is measured with the tank filled of water;
- The lowest roll period is measured in the case of a solid cargo. The difference between both measurements is of 23%, more than 2.5 seconds at full scale;
- The loading conditions with a viscous fluid are producing a roll period between the two previous values;
- A decrease of 70% of the viscosity between Day-1 and Day-2 is inducing an increase of 9% of the roll period, from T=1.66s to T=1.81s;
- The non-dimensional roll damping is about 10^{-3} in the solid configuration, 3.10^{-2} with water in the tank, and around 10^{-1} in the case of viscous fluid cargo.

Table 4. Free Decay tests analysis

Configuration	T(s) model scale	T(s) real scale
Solid	1.51	10.68
Water	1.86	13.15
Viscous Fluid – Day 1	1.66	11.74
Viscous Fluid – Day 4	1.81	12.80

The analysis of the free decay tests show that the nature of the cargo has a strong effect both on the roll natural period and on the ship roll damping. An increasing viscosity for the fluid in the tank is decreasing the roll period and tends to reach a limit equivalent to a solid cargo value. On the opposite, when the fluid has a low viscosity, the natural roll period is increased, the value obtained with water being certainly an upper bound.

The presence of a moving fluid cargo induces internal free surface effects, therefore decreases the value of the transverse metacentric height GM.

The loss of GM in these decay tests can be estimated from the following formula **Erreur ! Source du renvoi introuvable.** : $T_R = \frac{2.35R}{\sqrt{GM}}$, where T_R is the natural ship roll period, R is the radius of gyration in roll ($R = 0.34.B$, B being the breadth of the ship equals to 0.73m). The table below gives the GM value for each loading condition.

Table 5. Estimation of the GM

Configuration	T_R [s]	R [m]	GM [m]
Solid	1.51	0.2482	0.149
Viscous fluid - day 1	1.66	0.2482	0.123
Viscous fluid - day 4	1.81	0.2482	0.104
Water	1.86	0.2482	0.098

Based on these values, the stability of the ship is affected by the loss of GM and the risk of capsizing would increase as well with transverse seas. It should be however mentioned that the estimation is based on linear theory with the hypothesis of a (quasi-)static cargo.

Tests in regular waves

The following figures (Figures 5, 6 and 7) present typical time series of ship motions when the model is tested in a transverse regular wave of amplitude 0.02m and period of 1.27s (H=2m and T=9s at full scale). This wave period is chosen relatively far from the natural ship roll period. For each loading condition (solid, viscous, water), surge, sway then heave are shown in millimetres.

The surge motions are small values lower than 10mm confirming the model is correctly positioned transversally to the incident waves. The heave motions are also of the same order of the wave amplitude (20mm) and a stationary motion is reached after a certain number of waves (around 60).

The sway motions are shown on the middle graph of each loading condition figure. A transitory displacement (t=20s to t= 60s) is first observed then a low sway oscillation of roughly

35s period and 50mm amplitude is present related to the mooring stiffness.

The good repeatability of displacements during the tests, irrespective to the cargo nature, leads to assume the mooring is not affecting the rolling motion of the model.

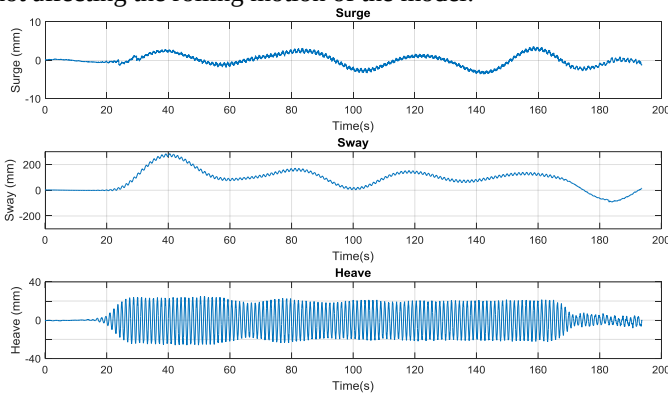

FIGURE 5. TIME SERIES FOR SOLID LOADING

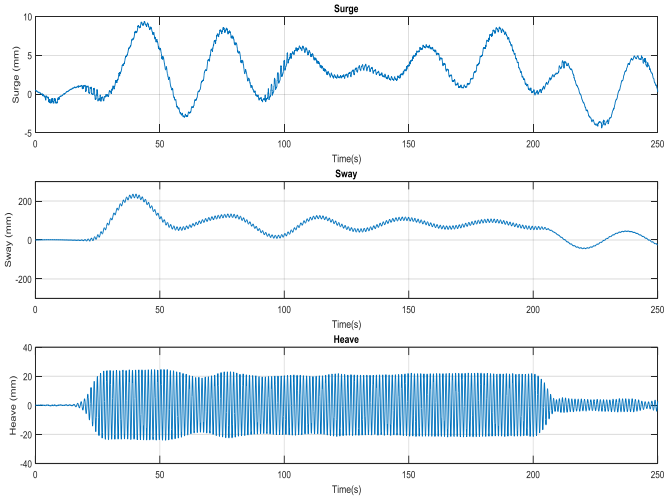

FIGURE 6. TIMES SERIES FOR VISCOUS LOADING

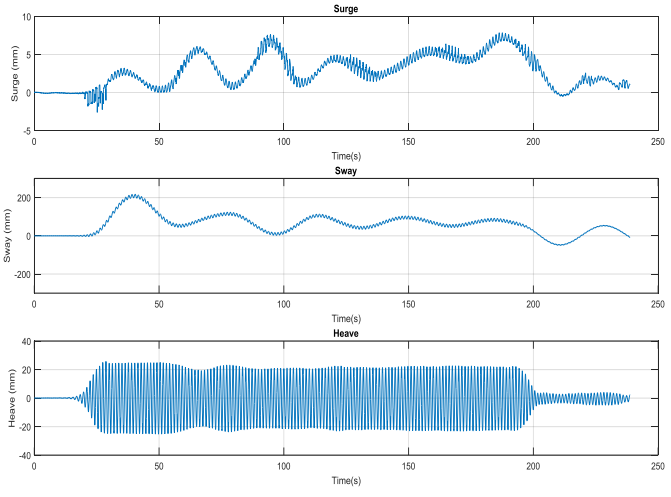

FIGURE 7. TIME SERIES FOR WATER LOADING

The following figure is reported the roll angles of the model during the same tests, with solid cargo (top graph), viscous cargo (middle) and fresh water (bottom)

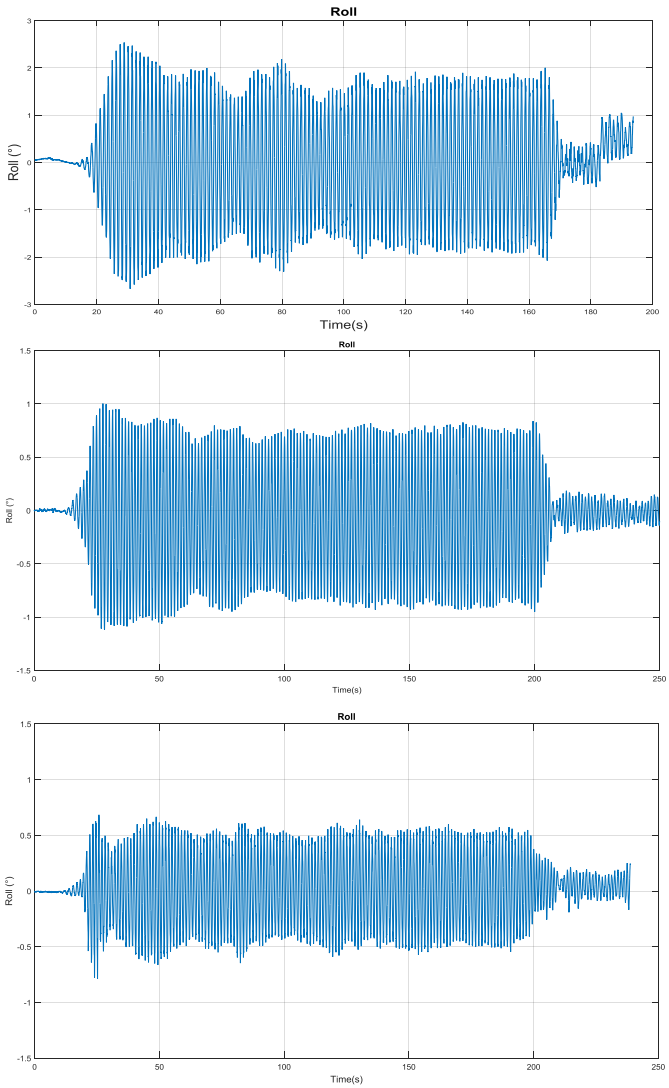

FIGURE 8. ROLL MEASUREMENT FOR (TOP) SOLID CARGO, (MIDDLE) VISCOUS CARGO AND (BOTTOM) WATER LOADING.

The nature of the cargo is influencing the roll motion of the model (for t>60s), with an average amplitude for the water loading approximatively a quarter of the angle measured with the solid loading (0.5° versus 1.8°). The viscous cargo is associated with a roll amplitude almost half way between the two loading conditions (around 0.8°).

The roll angles of the model at the respective natural ship roll period for each loading condition are reported in the Table 6 below and shown on the next figures. Note that to increase the visibility of the measurement, the viscous cargo results are shown for a wave amplitude twice than the one for the solid cargo.

Table 6. Roll measurements in regular waves

Loading configuration	Troll [s]	Roll amplitude[°]
Solid	1.51	15
Viscous liquid	1.72	2.5
Water	1.86	7.8

Regular waves with a period equivalent to the natural roll period of the ship generate resonance effects. This can be observed clearly for the solid cargo: higher amplitude would certainly induce capsizing. In case of a liquid cargo, the inner motion in the tank brings some damping to the ship motion. This effect is the strongest with a viscous liquid.

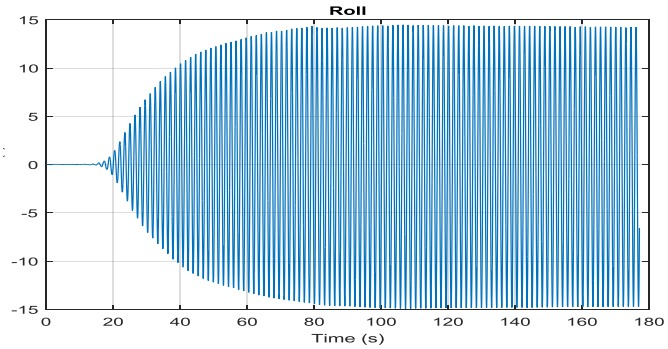

FIGURE 9. ROLL WITH SOLID LOADING, WAVE PERIOD 1.51S, AMPLITUDE 1CM

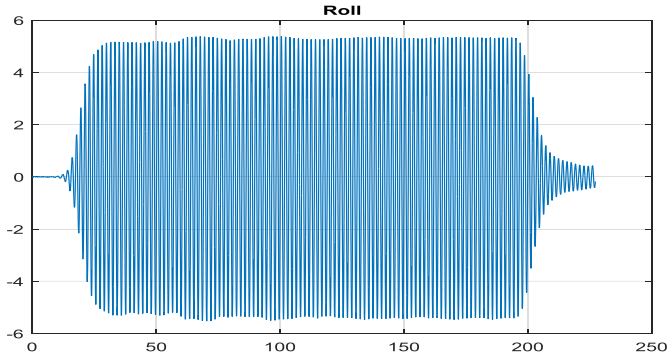

FIGURE 10. ROLL WITH VISCOUS LOADING, WAVE PERIOD 1.72S, AMPLITUDE 2CM

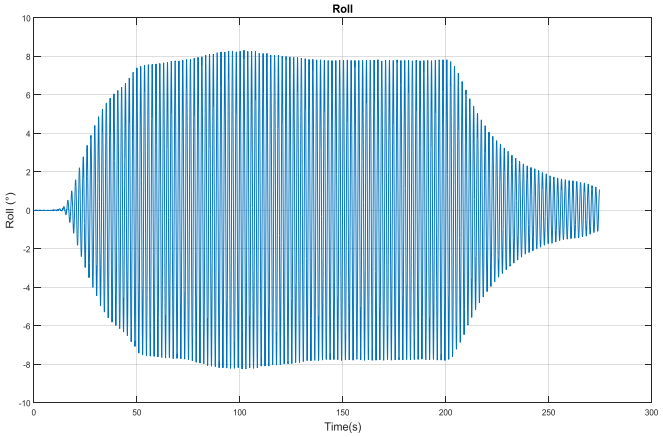

FIGURE 11. ROLL WITH WATER LOADING, WAVE PERIOD 1.86S, AMPLITUDE 1CM

Responses of the ship with regular waves

The incident wave amplitude of 20mm represents a risk of capsize for the solid loading and might be also dangerous with the fresh water. It is decided then to avoid this wave amplitude close the ship resonance period.

The FIGURE 12 below are presenting the Response Amplitude Operator (in °/cm) of the ship roll for regular waves of period from 0.8 to 2.5s and incident amplitudes of 1 and 2cm.

As seen previously, the resonance of the ship in roll is clearly reached at T=1.51s for the solid loading and T=1.86s for the water loading.

A second small peak is however seen around 1.1s in this configuration. The theoretical sloshing period would be 1.2s for a rectangular tank, with same overall dimensions and filled with 0.135m of water. As the theoretical period would be a bit smaller with a prismatic bottom, it is assumed that this experimental peak is the (water) sloshing period of the tank.

An increased incident wave amplitude is not changing the response (apart from the resonance area) for the solid and water loadings. At least for these amplitudes, the linear approach is valid.

For the viscous cargo, the behaviour is different. Globally the curve of the response is flatter without strong peak. The range of period with roll amplification is quite large, from 1.4s to 2s, while the level of response stays relatively low (<3°/cm). The fluid damping associated with the viscosity of the cargo is influencing response of the ship.

The viscous liquid is showing however a non-linear behaviour as the 10mm incident wave amplitude generates a higher response than the 20mm incident amplitude. Some more specific analysis is necessary to understand this point especially related to the inner motion in the tank.

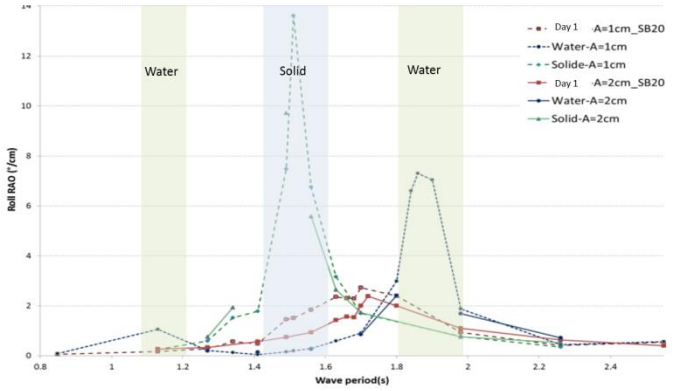

FIGURE 12. RAO IN ROLL FOR THE 3 LOADING CONDITIONS (SOLID, VISCOUS LIQUID AND WATER)

As mentioned previously, the stability with the time of the viscous fluid is not assured. From the day 1 to the day 5, the viscosity of the liquid is decreasing, without noticeable change in density. The FIGURE 13 is summarising the roll RAO obtained during these testing days with the viscous loading.

The roll resonance period is increasing with the decrease of viscosity, as noticed with the decay tests results. It tends to reach the period corresponding to the fresh water, around 1.8s – 1.9s.

The attenuation of the response is however increasing in the same time. This behaviour is not obvious as we would presume that the mixture disintegration should tend to a water-like behaviour with a strong peak response at a period around 1.8s. This flat response may be caused by an increase of the surface tension counterbalancing a lower viscosity and preventing the sloshing effect in the tank. The fluid free surface might be then almost still and the ship response would be similar to the solid loading condition at this period. As the surface tension was not measured during this experimental campaign, the hypothesis has to be verified.

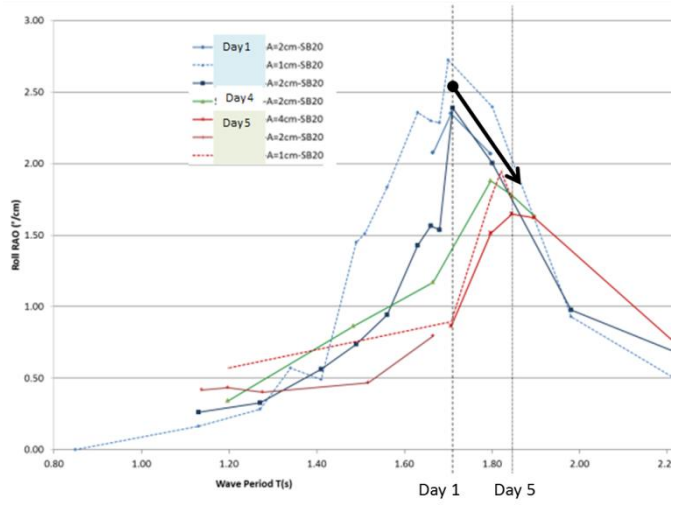

FIGURE 13. EVOLUTION OF THE ROLL RESPONSE WITH A VISCOUS LOADING CONDITION AND A DECREASING VISCOSITY WITH TIME.

The measured viscosities of the liquid in the tank are of the same order than the Nickel ore slurry of 40% and 50% mentioned in [6]. This slurry can be obtained either after a badly drained loading of the holds (situation forbidden by the IMSBC code) or after a cargo liquefaction occurring on the route. A bulk carrier filled with these types of slurry would then present some roll RAO characteristics similar to the present experiment.

In particular medium to high transverse (irregular) waves may generate a ship roll response both at periods higher than the "solid" loading resonance and with a noticeable amplification compared to a regular bulk cargo. This configuration would be at least critical for the ship and maybe dramatic for the crew if leading to capsizing.

Internal fluid behaviour

This section is dedicated to the free surface evolution measured in the tank of the ship, in the water loading condition and in the viscous liquid loading (especially with the high viscosity of day 1). The different wage gauges are located in the tank according to the sketch of FIGURE 3.

An illustration of the signals from the wave gauges is given by the FIGURE 14 with an incident wave of 1.8s and 0.02m amplitude, for the water loading condition.

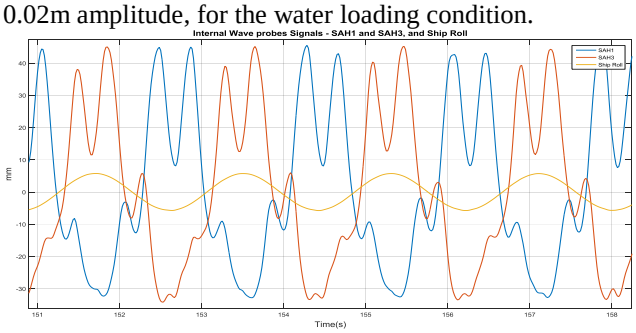

FIGURE 14. TANK WAVE MEASUREMENTS WITH WATER LOADING, T=1.8s A=0.02m

The FIGURE 15 shows the maximum amplitude of the wave gauges with the water loading condition. Two peaks are present. The first at a period around 1.1s is the already mentioned sloshing period of the tank. The second peak at 1.86s is the natural ship roll period.

Strong motions of the free surface are observed with wave heights of 40mm and some measurements by the wave gauges are not possible due to braking waves and ventilation.

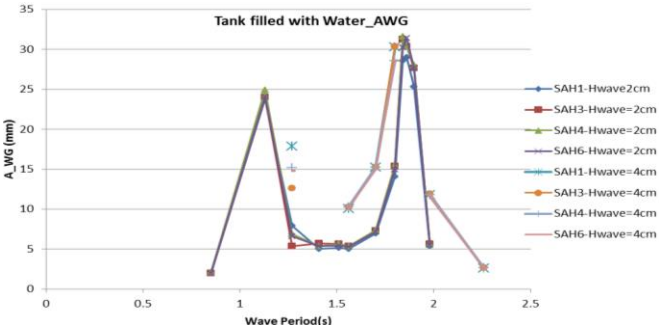

FIGURE 15. TANK WAVE RESPONSES WITH WATER LOADING

A similar graph is given FIGURE 15 for the viscous loading condition. The highest amplitudes of the free surface are only observed at the ship roll period. The amplitudes are however almost halves those from the water loading results.

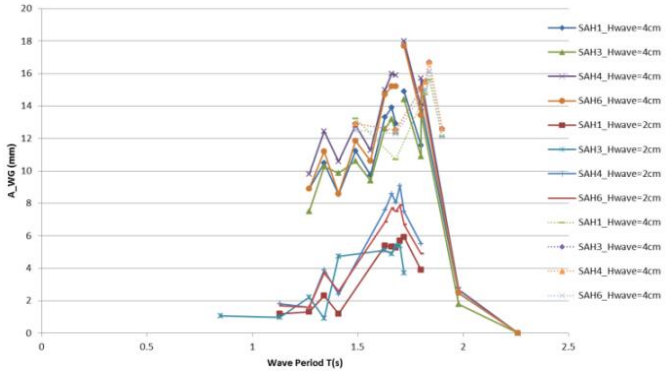

FIGURE 16. TANK WAVE RESPONSES WITH VISCOUS LOADING

FIGURE 17 presents the shape of the free water surface at 4 different instants for an incident wave period of 1.13s and 0.01m amplitude. The far left and the far right parts of the curve are at 0.15m of the respective lateral tank walls. According to the slopes, the free surface is assumed to hit the top of the tank in the upper corners.

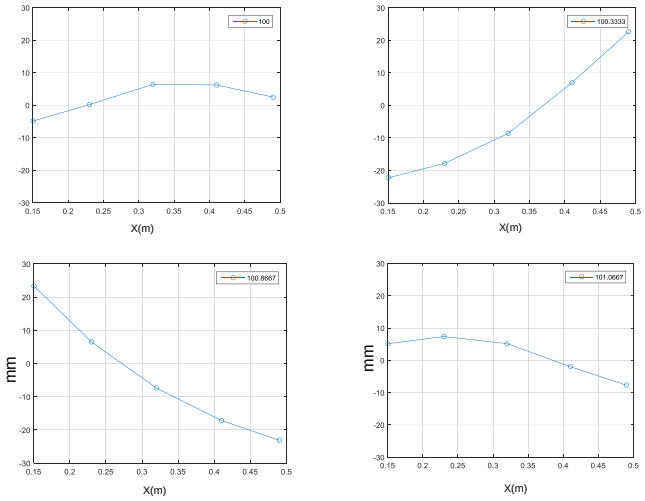

FIGURE 17. WATER LOADING: LOCATION OF THE FREE SURFACE FOR A WAVE PERIOD T=1.13S, A=1CM

The difference with the viscous liquid is noticeable when compared with the FIGURE 18 for the same wave conditions. The cargo is almost not moving and keeps a still free surface. The inner damping is attenuating the motions of the fluid and there is no interaction with the ship hull.

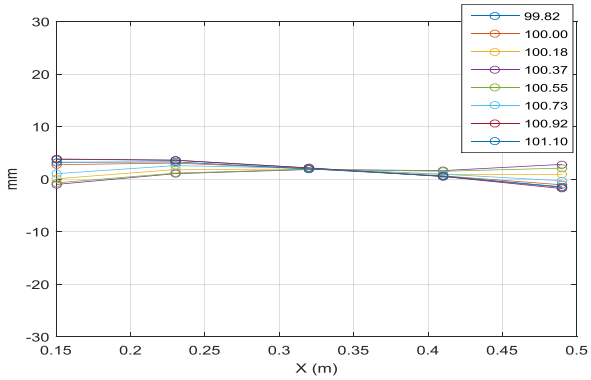

FIGURE 18. FREE SURFACE PROFILE FOR VISCOUS LOADING, T=1.13S, A=1CM

Close to the viscous loading resonance, i.e. T=1.68s, the shape of the free surface given by FIGURE 19 presents a node at the centre of the tank. The shape of the liquid is similar to an oscillating flat surface. The linear standing wave is oscillating between +10° and -10° around a node which is also higher than the still elevation of the fluid.

The following **Erreur ! Source du renvoi introuvable.** presents the temporal evolution of the free surface measured by the wave gauges, with an incident wave of period 1.72s and 0.02m amplitude. The crests are clearly flattened and the mean level of the fluid is slightly higher than the resting level.

These observations are similar to the reported measurements from the forced motion tests reported in [8]. Smooth free surface profile evolutions are also obtained numerically by Zhang & al for a Nickel ore slurry with a viscosity close to the present viscous fluid [7].

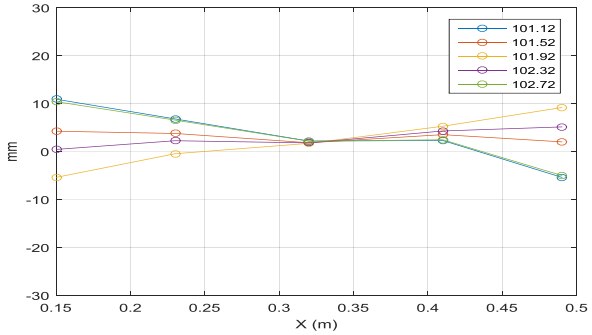

FIGURE 19. FREE SURFACE PROFILE FOR VISCOUS LOADING, T=1.68S, A=1CM

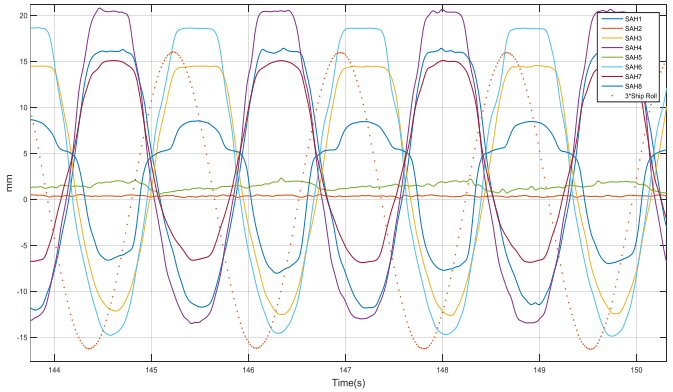

FIGURE 20. FREE SURFACE MEASUREMENTS IN THE TANK WITH VISCOUS CARGO, T=1.72S, A=0.02M

The experiments on the hexapod [8] have shown phase lags between the motion of the tank one hand and the fluid motions with the associated global loads, on the other hand. The figures below are trying to describe such behaviour, i.e. focusing on the phase lag between the motion of fluid seen by the wave gauges close to the lateral tank wall (WG1 and WG4) and the roll motion of the ship.

In the case of water loading condition (FIGURE 21) and according to the definition of phases, the figure below shows that the cargo is moving in phase with the ship for periods higher than the natural ship roll period with a solid cargo (T=1.51s). For small wave periods, the motion of the free surface is opposite to the ship roll and the phase lag is null.

The FIGURE 22 is illustrating the position of the free surface in the tank related to the position of the ship. A phase lag of 180° is equivalent to have the water cargo moving naturally with the tank: the mass of the cargo is flowing towards the low side and the free surface tends to stay horizontal irrespective to the position of the ship.

A zero phase lag for the low periods is indicating that the mass of the fluid is moving in the opposite way: the water run-up is maximum on the elevated side of the tank (ship righting herself).

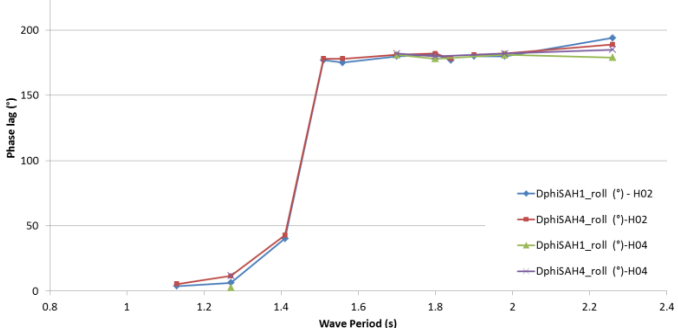

FIGURE 21. PHASE LAG WITH WATER LOADING

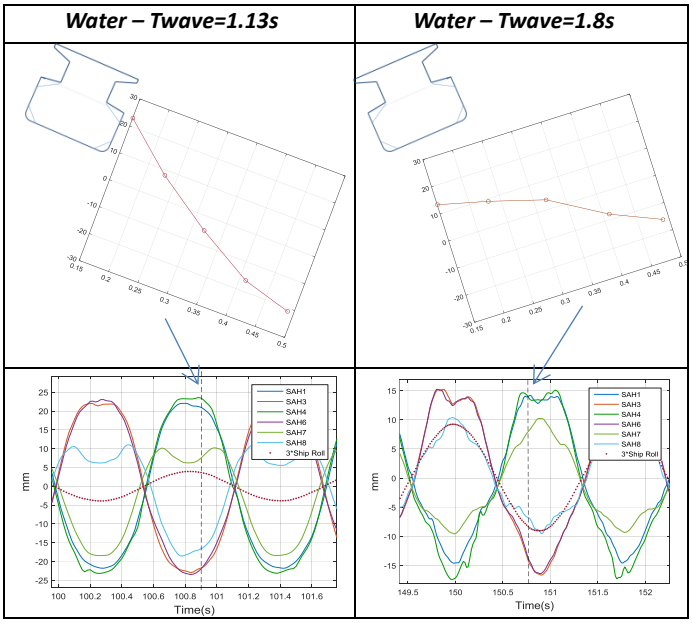

FIGURE 22. FREE SURFACE GLOBAL PROFILE AND CORRESPONDING ROLL MOTION TWAVE=1.13S (LEFT), AND FOR TWAVE=1.8S (RIGHT) WITH WATER LOADING

In the viscous loading case, the FIGURE 23 is showing the evolution of the phase lag with two viscosities. The lower viscosity presents an evolution towards the water case: low value of phase lag then almost 180° over 1.6s of wave period (square and triangle symbols).

The phase lag associated with a high viscosity (day 1) is showing an unique evolution with the wave period with values to 70° to 135°. The phase lag is also different with respect to considered wave gauge: 8 to 12° of difference are measured between WG1 and WG4 even if they are at the same distance from the portside lateral wall.

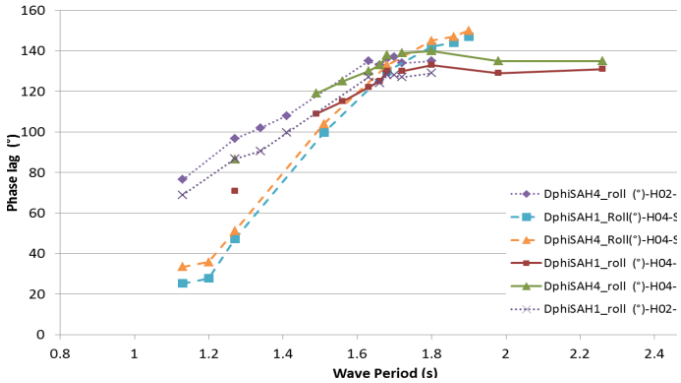

FIGURE 23. PHASE LAG WITH VISCOUS LOADING

Globally the motion of the viscous cargo is more complex than the case of water loading as there is always a phase lag between the roll and the movements of this fluid. The ship roll is therefore affected by the inner viscous motion and this one is a result of low velocities and dissipation effects (internal fluid damping). As an example, fluid accumulation may occur on a ship side and generate an additional inclining moment which may be favourable or not to the ship stability.

The FIGURE 24 below illustrates the existing phase lag between wave gauges and roll angle of the model. Further analyses are needed to understand the interaction between inner viscous motion and roll motion.

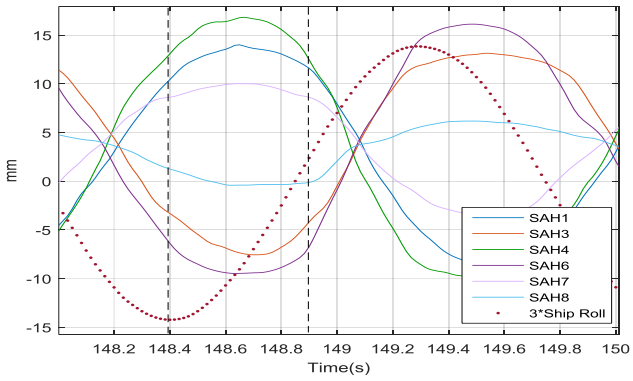

FIGURE 24. FREE SURFACE MEASUREMENTS IN THE TANK WITH VISCOUS CARGO, T=1.8S, A=0.02M

CONCLUSION

The liquefaction of some mineral ore may lead to the capsizing of a bulk carrier but the physical mechanism is not well understood. To explore the interaction between a viscous fluid simulating a liquefied cargo and a rolling ship, experiments are performed in a wave tank with a simplified model.

The responses of the model under transverse regular waves show a complex feature with a fairly large range of wave periods inducing roll motions and a strong effect of the viscosity damping on the amplitudes.

Phase lags between ship motions and inner fluid motions are also highlighted but additional studies are needed to fully understand these interactions.

ACKNOWLEDGMENTS

The work presented in this paper has been funded by the French ministry of Ecology, Sustainable Development and Energy. We also acknowledge the members of the LiquefAction project consortium, and especially Oldendorff carriers.

REFERENCES

[1] Munro Michael C., Mohajerani A., "Bulk Cargo liquefaction incidents during marine transportation and possible causes", Ocean Engineering 141 (2017)

[2] IMO International Maritime Solid Bulk Cargoes code (IMSBC)

[3] GARD AS : Liquefaction of solid Bulk Cargoes – http://www.gard.no/Content/20651223/Cargo

[4] IMO - Iron ore Technical Working Group –Marine report

[5] Zou Y., Shen C., Xi X., "Numerical Simulations on the Capsizing of Bulk Carriers with Nickel Ores", The Journal of Navigation (2013), 66;

[6] Zhang J., Wanqing W., Junquan H., "Parametric studies on nickel ore slurry sloshing in a cargo hold by numerical simulations", Ship and Offshore Structures 2017, Vol.12

[7] Zhang J., Wanqing W., Junquan H., "Study on the sloshing of nickel ore slurries with three different moisture contents", JOMAE, June 2017, Vol.139

[8] Baudry V., Rousset J.M., "Experimental study of viscous cargo behavior and investigation on global loads exerted on ship tanks", Proceedings of OMAE 2017 conference, June 2017, Trondheim, Norway

[9] Zhao W., Efthymiou M., McPhail F., Wille S., "Nonlinear roll damping of a barge with and without liquid cargo in spherical tanks", Journal of Ocean Engineering and science 1 (2016)